Independent Benthic Microbial Fuel Cells Powering Sensors and Acoustic Communications with the MARS Underwater Observatory

PAUL S. SCHRADER AND CLARE E. REIMERS

Hatfield Marine Science Center, College of Earth, Ocean, and Atmospheric Sciences, Oregon State University, Newport, Oregon

PETER GIRGUIS AND JENNIFER DELANEY

Biological Laboratories, Harvard University, Cambridge, Massachusetts

CODY DOOLAN

Hatfield Marine Science Center, College of Earth, Ocean, and Atmospheric Sciences, Oregon State University, Newport, Oregon

MICHAEL WOLF AND DALE GREEN

Teledyne Benthos, Inc., North Falmouth, Massachusetts

(Manuscript received 6 May 2015, in final form 9 November 2015)

ABSTRACT

Most oceanographic instruments on the seafloor have no connections with the surface and therefore have to run on batteries and store data until recovery. To demonstrate a developing technology, sensors and acoustic modems were powered with energy harvested from the seafloor, and data were relayed acoustically in near–real time to the Monterey Accelerated Research System (MARS) observatory in Monterey Bay, California, and to surface research vessels. MARS is a cabled observatory in deep water (~890 m) at the edge of Monterey Canyon. An acoustic modem was attached to the MARS node and configured to send out commands to, and relay data received from, remote modems. Two benthic microbial fuel cells (BMFCs) positioned approximately 0.5 km away from MARS supplied power to the remote modems and sensors. At their peak performance, these BMFCs produced continuous power densities of ~35 mW m^{-2} (footprint area). The modems utilized in this study contained an integrated power management platform (PMP) designed to manage and store the electrical energy generated by each BMFC and to record BMFC performance parameters and sensor data on an hourly basis. Temperature and either oxygen or conductivity sensors were chosen because of their common use and environmental relevance. Acoustically transmitted data records show that the BMFCs renewed energy stores and that the oceanographic sensors measured dissolved oxygen, temperature, and conductivity reliably throughout the operational life of each BMFC system (~6 months). These systems remained in place for more than 12 months.

1. Introduction

The first functional prototypes of benthic microbial fuel cells (BMFCs) were constructed just 14 years ago (Reimers et al. 2001; Tender et al. 2002). BMFCs are bioelectrochemical devices driven by the potential difference between anoxic sediment and oxic seawater. Electrons are delivered to the anode either from organic material or inorganic products of organic matter degradation serving as "fuel" (Reimers et al. 2007). These electrons travel along a wire connecting the anode to the cathode, thereby generating an electrical current and reducing dissolved oxygen to form water at the cathode. Microorganisms play several roles in these systems, including the: maintenance of the redox gradients, production of redox-active mediators, generation of

Corresponding author address: Paul S. Schrader, Hatfield Marine Science Center, College of Earth, Ocean, and Atmospheric Sciences, Oregon State University, 2030 S.E. Marine Science Dr., Newport, OR 97365.
E-mail: paul.schrader@oregonstate.edu

DOI: 10.1175/JTECH-D-15-0102.1

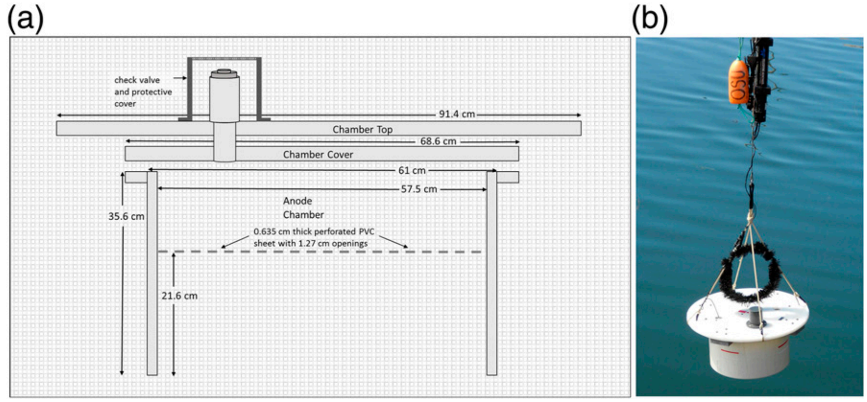

FIG. 1. (a) Engineering drawing of the BMFC chamber deployed at the MARS observatory. (b) Image of assembled BMFC chamber prior to test in Yaquina Bay, Oregon. The cathode is directly above the chamber. Above the cathode is the acoustic modem and PMP housing with an oxygen optode sensor attached to the side, all suspended by the foam float.

electron-rich metabolites (e.g., sulfide ions) and, in some cases, delivery of electrons to an electrode through direct electron transfer (Bond and Lovley 2003; Holmes et al. 2006; Lovley 2006; Reguera et al. 2006).

BMFCs are promising power sources for a variety of marine sensors that have low power requirements and that have been designed to rely on batteries (Reimers 2015). There are several major drawbacks to battery power, including the limited lifetime of batteries in the cold deep sea, the high cost of periodic servicing via remotely operated vehicle (ROV) or other seagoing assets, and the risk of losing valuable data if stored records are not retrieved until the instrument is recovered. These challenges are especially acute in deep-water deployments.

In the past 10 years of development, BMFCs have typically exhibited continuous power densities of 1–10 mW m^{-2} (with areas representing chamber or simple plate electrode footprint) during testing in a wide variety of marine environments (Bond et al. 2002; Gong et al. 2011; Nielsen et al. 2007; Reimers et al. 2001; Tender et al. 2002, 2008; Wotawa-Bergen et al. 2010). The peak power densities of these BMFCs have ranged from 10 to 30 mW m^{-2}. Under less common operational conditions, such as when a BMFC was deployed at a methane cold seep or a hydrothermal vent, peak power densities as high as 380–500 mW m^{-2} have been observed (Girguis and Holden 2012; Nielsen et al. 2007, 2008).

To date, BMFCs have only just begun to be applied to power a range of environmental sensors and thus to prove themselves as a viable means of providing long-term uninterrupted power for marine devices (Donovan et al. 2008; Gong et al. 2011; Tender et al. 2008; Wotawa-Bergen et al. 2010). The objective of this study was to demonstrate BMFC-powered underwater sensing/acoustic communications in conjunction with the deep-sea scientific research infrastructure at the Monterey Accelerated Research System (MARS) observatory in Monterey Bay, California. Two BMFC systems were used to harvest energy, collect sensor data, measure fuel cell performance metrics (e.g., daily polarization curves, and response to acetate supplements), and power an acoustic modem used to transmit the data to either the MARS observatory or a surface vessel. This is the first long-term deep-water deployment demonstrating the ability of a BMFC to supply energy to sensors in an inhospitable environment. It is also the first time a BMFC has been used to remotely communicate with an installed scientific research platform via acoustic transmissions, demonstrating the possibility of real-time remote data networking. Sediment properties and microbial communities were also characterized, as previous studies have shown striking differences in BMFC performance among different locations due to these variables (Dewan et al. 2010).

2. Materials and methods

a. BMFC, acoustic modem, power management platform, and sensor systems

Identical cylindrical chambered BMFCs were fabricated in duplicate (Accelerate, Inc.; Fig. 1). Each chamber was constructed of polyvinyl chloride (PVC; 0.36 m high × 0.57 m diameter with an open bottom; 0.259-m^2 footprint). The chamber was designed such that the lower 60% of the volume could be submerged in the sediment while the upper volume, separated by a 0.6-cm-thick perforated PVC screen, housed the anode just above the sediment in an anoxic environment. The perforated screen was intended to create a physical barrier to bioturbating organisms that could burrow under the chamber and aerate the seawater surrounding the anode. A solid PVC top was bolted onto the chamber and sealed with a Viton rubber gasket. The top contained a one-way check valve (Plast-O-Matic Valves, Inc.) to prevent the buildup of pressure and to allow water to exit the chamber during descent. The anode and cathode electrodes were constructed using twisted #11 titanium stem wire and Panex 35 carbon fiber fill brushes with 400 000 tips per inch intertwined in the titanium stem wire (Mill-Rose). Each anode was 4 m in length, while each cathode was 2.2 m in length, in keeping with previous findings that the cathode can be at least 0.5 times the length of the anode without the reaction at the cathode becoming rate limiting (Gong et al. 2011). A jacketed wire was run from the anode through the top of the chamber in a watertight fitting to a breakout cable that was also wired to the cathode. The other end of this cable connected to the modem housing and an internal power management platform (PMP). The purpose of the PMP was to monitor, harvest, store, and shunt the electricity generated by the BMFC to the sensors and modem.

To test the effect of exogenous carbon on start-up time and power production, four 1-L gelatin blocks containing 200 mM of acetate were added to each of the anode chambers of both BMFCs. The blocks were placed in mesh bags and attached to the inside of each chamber prior to deployment. The concentrations were chosen to sustain an acetate concentration of ~10 mM inside each anode chamber as the blocks dissolved.

Each BMFC was also equipped with two osmotically powered pumps (or osmopumps) attached to the top of the chamber lid and joined to an ~300-m-long coil of tubing with the open end inserted into the anode chamber (Jannasch et al. 2004). These pumps were used to sample and preserve the fluid from within the benthic chamber over time, without the use of electrical power. One osmopump was equipped with 12 membranes (designed to facilitate the withdrawal of fluid from the chamber continuously at a rate equal to approximately 1 mL day^{-1}), and the second osmopump was equipped with one membrane to deliver a stock solution of 360 mM high-purity trace metal clean HCl to the sample coil (at a rate expected to yield a final acid concentration of 30 mM). The tubing was initially filled with 0.2-μm filter-sterilized distilled water, which was displaced by the sample as fluid was drawn from the anode chamber. Upon recovery, the OsmoSampler coils were detached from each BMFC and stored at 4°C until sectioning, which was done within 2 days. The sample coils from both BMFCs were sectioned in 1-m increments, each representing samples drawn over 1.4–2 days. Decanted fluid was stored at 4°C until analysis. Every other 1-m section was used to determine acetate concentrations in the chamber fluid by colorimetric assay [acetic acid (acetate kinase analyzer format); Megazyme International]. The remaining 1-m sections were used for chemical analysis via inductively coupled plasma atomic emission spectroscopy (ICP-AES) as in Wheat et al. (2010).

The energy harvested from any BMFC will be at low voltage (<0.8 V), impractical to power most solid-state devices. In this study, this energy was directed to the PMP, which was a custom-designed circuit board housed within the compact acoustic modem (both Teledyne Benthos products). The PMP consisted of a multistage boost converter, a 2-V supercapacitor, and a programmable microcontroller with circuits and firmware to monitor and optimize energy storage and usage in real time. The boost converter was designed to charge two 3.7-V lithium-ion (Li-ion) batteries, which were connected in series and in turn provided 5 V for an application sensor and 7 V for the acoustic modem. An oxygen optode/temperature sensor was used on one BMFC and a salinity/temperature sensor on the other (Aanderaa models 4330 and 4120BIW, respectively). The microcontroller managed daily scheduled potential sweeps (i.e., polarizations controlled by varying the resistance stepwise from 10 000 to 5 ohms between the anode and cathode), hourly sensor readings, and power for the acoustic modem. The purpose of the potential sweeps was to determine the current (I) − voltage (V) characteristics of the BMFC.

The compact acoustic modems (model ATM-925) transmitted data at a rate of 430 bits s^{-1} with an omnidirectional toroidal beam pattern in the low-frequency range of 8.96–14.08 kHz. In addition to the sensor data (temperature and dissolved oxygen or salinity), the voltage of the supercapacitor, and whole cell voltage (the voltage difference between the anode and cathode) were recorded on an hourly basis and available for transfer. The data collected were stored in a 14-day circular memory buffer in the modem. These data were available to be transmitted acoustically in packets of 1–14 days after receiving an acoustic command from either the surface (on a nearby ship) or the MARS observatory. Most often, 7–8-day packets were requested per transmission so as to minimize the power demand and the possibility of transmissions being interrupted.

b. *MARS observatory, equipment deployment, and recovery*

MARS is a cabled observatory that sits in deep water (~890 m) at the edge of Monterey Canyon (latitude

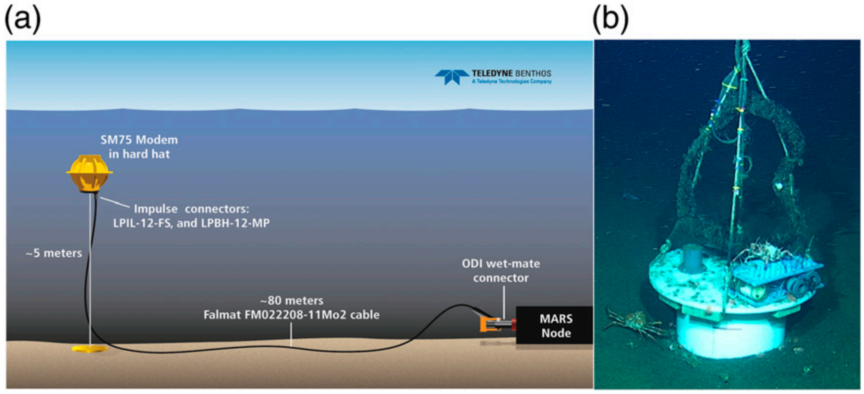

FIG. 2. (a) Illustration of the MARS observatory "science node," which has eight ports to supply data and power connections for a variety of scientific instruments, and a cable to shore-based facilities to allow scientists continuous access to their equipment and experiments. (b) A BMFC deployed 0.5 km from the MARS observatory.

36.712 508, longitude −122.186 757) about 23 mi seaward of the Monterey Bay Aquarium Research Institute (MBARI; available online at http://www.mbari.org/mars/general/about_mars.html) (Fig. 2). It provides a site for researchers to test ocean-observing equipment and to design experiments dependent on a regional observing network. Science instruments can be attached to the observatory node using underwater data/power connectors and extension cords up to 4 km long. The MARS node has electronic equipment that converts a 10 000-V power source supplied from the shore to 375- and 48-V (dc) outputs routed to eight science ports.

In this experiment, a Teledyne Benthos Smart Modem Acoustic Release Technology (SMART) modem (SM) 75 was attached on 27 October 2011 to a 48-V port via the ROV *Ventana* operated from the R/V *Point Lobos.* The SM75 was configured to relay data received from remote modems back through MARS to scientists' computers onshore. Scientists, in turn, were able to send commands out from MARS to request data transmissions from the compact modems on the BMFC-powered packages. However, grounding problems with the modem attached to the MARS node and associated acoustic interferences necessitated that initial data recovery efforts instead be from ships operating near the site using a Universal Deck Box and transducer (Teledyne Benthos). Ultimately, another high-power modem (Teledyne Benthos) was deployed on 15 May 2012 (latitude 36.712 225, longitude −122.182 826; 876-m depth) to serve as a relay between the compact modems on the BMFCs and the modem attached to the MARS node.

The modem/sensor/BMFC packages were deployed from a surface vessel on 15 November 2011 using a system of releasable "elevator" floats to slow descent to the seafloor at locations approximately 0.5 km away from the MARS node (BMFC 1: latitude 36.715 073, longitude −122.183 237; BMFC 2: latitude 36.709 230, longitude −122.182 677), and at depths of 863 and 895 m. The ROV *Ventana* was used to release the elevator floats and to ensure BMFC chambers were inserted into the sediment.

The ROV also collected sediment core samples from each BMFC deployment site soon after deployment. At recovery nearly a year later (13 November 2012), core samples were again collected targeting sediments exposed after each BMFC chamber was picked up. All cores were sectioned into 2-cm increments once back onshore, and these samples were placed in individual Whirl-Pak bags and frozen for future laboratory analysis. Subsamples were subsequently taken from each section, freeze-dried, and analyzed for nitrogen and organic carbon content using an elemental analyzer (Hedges and Stern 1984).

The BMFCs were recovered on 13 November 2012 by ROV, approximately 12 months after deployment. Postrecovery, carbon fiber anode and cathode samples were taken immediately upon receiving each fuel cell on board the R/V *Rachel Carson* by clipping carbon fibers with sterile scissors at random locations along each brush. Each sample was placed in individual Whirl-Pak bags and frozen. DNA was later extracted from a representative anode subsample and from a representative sediment subsample from the uppermost centimeter of sediment recovered from under BMFC 2 at the time of recovery. Total genomic DNA was obtained using the PowerSoil DNA Isolation Kit (MoBio Laboratories) following the manufacturer's protocol with the added cell lysis procedure consisting of heating the sample to 60°C followed by three cycles of intermittent bead beating for 60 s and chilling on ice for 60 s. DNA was collected and stored in 10-mM Tris. Each DNA sample was quantified using a Quant-iT dsDNA High-Sensitivity (HS) Assay Kit and Qubit fluorometer (Invitrogen).

DNA amplification and sequencing were performed by an outside laboratory (Research and Testing Laboratory). 16S rRNA genes were amplified by polymerase chain reaction (PCR) using 28F (5′-GA GTT TGA TCM TGG CTC AG-3′) and 519R (5′-GWA TTA CCG CGG CKG CTG-3′) primers (Nielsen et al. 2008) that are designed to target bacterial rather than eukaryotic or archaea communities. Amplicons were sequenced using 454 titanium pyrosequencing technology (454 Life Sciences). Microbial community analysis was performed on these samples through sequencing 16s rDNA as described previously (Reimers et al. 2013). In brief, raw sequence data were analyzed using the Quantitative Insights into Microbial Ecology (QIIME) 1.4.0 software package (Caporaso et al. 2010). Chimera were then detected and filtered out using UCHIME. Taxonomic assignments were given to those sequences retained using first the Ribosomal Database Project (RDP) classifier (Wang et al. 2007) and then using the Basic Local Alignment Search Tool (BLAST; Altschul et al. 1990) for those not successfully classified with RDP. The purpose of these analyses was to determine what bacteria were likely to have contributed to processes of electron shuttling to the anode.

c. *Energy budget calculations*

Following the approach of Gong et al. (2011), an energy budget was derived for each BMFC/sensor/modem system. Accordingly, EBMFC is the energy harvested from the microbial fuel cell. This is calculated as the product of an average daily fuel cell potential (derived from hourly records) and current (giving power), and time. In this study, current estimates were interpolated from daily polarization curves.

Measurements of energy flows and losses through the PMP hardware were made following recovery from Monterey Bay before making any changes to the units. The three major performance measures analyzed were baseline power consumption, secondary charge pump efficiency, and primary charge pump efficiency. The block diagram in Fig. 3 illustrates the electrical flow of the PMP.

Baseline power consumption was defined as the average power consumption by the microcontroller simply running and controlling the charge pumps. A variety of known currents were injected into the MID point while measuring voltage changes on the 100F and 5F capacitors. Baseline power consumption ranged from 0.70 to 0.75 mW.

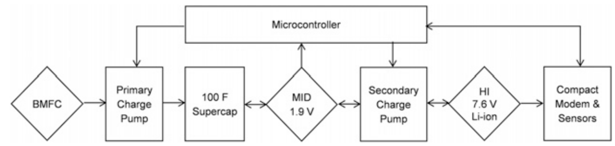

FIG. 3. Block diagram illustrating the flow of electricity from the BMFC through the PMP, including the microcontroller.

The efficiency of the secondary charge pump was measured by injecting a variety of known currents into the MID point while a known resistance was placed on the HI point to determine where the capacitors maintained constant charge. The secondary charge pump efficiency was determined to be at least 98% at the power levels observed in this study.

The primary charge pump efficiency was measured by injecting a variety of known currents into the microbial fuel cell (MFC) point while a known resistance was placed on the MID point to determine where the capacitors maintained constant charge. At low-power levels (~1 mW), the efficiency of the primary charge pump was observed to be at least 98%. Efficiency decreased with increasing power levels, such that it was ~80% at 9.2 mW. The efficiencies are a function of the size of the capacitor, the relative charge difference between the fuel cell and the capacitor, and the settings used to determine when the primary charge pump cycles.

The following equations were used to partition and report energy production by each BMFC in this study:

$$\text{Euseful} = \eta 1 \eta 2 \text{EBMFC}, \tag{1}$$

where $\eta 1$ is the efficiency of the primary charge pump converter on the power management board (conservatively equated to 80%) and $\eta 2$ is the efficiency of the boost converter, or secondary charge pump (equated to 98%; see above). And,

$$\text{Econs} = \text{Emq} + \text{Ebq} + \text{Etrans} + \text{Eoptode}, \tag{2}$$

where Econs is the energy consumption and is the summation of Emq, the energy needed to maintain the acoustic modem in a quiescent state (derived from a power consumption rate = 3 mW); Ebq is the minimum energy required to maintain the duties of the power management platform, including the internal clock (estimated to require a constant 0.75 mW); Etrans is the energy consumed whenever the acoustic modem was activated and remotely transmitted stored data from the deployment site to shore; and Eoptode is the energy consumed by the oxygen optode or conductivity sensor for hourly readings (each = 250 mW × 3 s = 0.75 J). During this experiment, daily values of Etrans ranged from 0 to 234 J) being dependent on if and how many data packets were retrieved. The modem power level was set at 8 (maximum power), and 40 J were estimated to be consumed per kilobyte with one day's data equaling 1.1 KB.

Enet is the net daily energy saving and is defined as the difference of Euseful and Econs:

$$\text{Enet} = \text{Euseful} - \text{Econs}. \quad (3)$$

It is important to note that the compact modem/PMP connected to each BMFC contained two 3.7-V Li-ion batteries that were nearly fully charged at the time of deployment. These batteries were used to sustain operations while the BMFCs came up to power, after which they were recharged using excess energy produced by the BMFCs.

3. Results

a. BMFC deployment and site characterization

Initial free-fall deployment of the BMFC systems went smoothly as these assemblies landed at their desired locations intact and in the proper orientation. However, each BMFC chamber did not appear to be submerged very deeply into the sediment. All efforts by the ROV pilots to insert the fuel cells further into the sediment were met with resistance and resulted in only modest gains with both chambers being less than 10 cm deep (ideal depth ~20–30 cm). Sediment core samples collected from each site soon after deployment revealed a compact clay deposit just centimeters below the sediment surface that likely impeded insertion of the BMFCs. This resulted in less sediment within the chamber and a greater-than-desired proportion of the chamber volume consisting of seawater. A large water volume is expected to require more time and microbial activity to create an anoxic environment and thereby a favorable redox gradient for energy harvesting. Further analysis of the sediment core samples showed the sites to be organic poor with the total organic carbon content of the solids $\leq 1\%$ dry weight.

b. Modem communications

Following deployment, attempts at communicating with the BMFC systems through the modem attached to the MARS node were problematic. It was evident that the remote compact modems were receiving the query commands but the responses were unintelligible. Commands were sent to these modems to maximize the power of their transmissions but resulted in no improvement. An acoustic path refraction analysis was subsequently performed with models indicating only 1 m of bending given the recorded sound velocity profile over the ~500-m distances between the MARS node and BMFC systems, thereby eliminating refraction as the problem. Communication with the BMFC compact modems and data recovery were initially established on a ship via surface hydrophone. This was fortuitous in so far as it both displayed the ability to communicate with the BMFC systems in deep water from a surface vessel and indicated the problem was with the SM-75 modem attached to the MARS node. It was discovered that a seawater return for power was required for proper grounding of the SM-75, but this ground had not been established, resulting in noisy data reception. Data continued to be collected intermittently via surface hydrophones from ships sent to the area, until another high-power modem was deployed at the site to strengthen the signal and act as a relay between the BMFC systems and the MARS node. The relay modem was deployed 182 days after deployment of the fuel cells. This solution resulted in good communications between MARS and the remote modems for the remainder of the BMFC systems' activities.

c. Data collection and energy production

While the acoustic modems powered by the microbial fuel cells performed as expected, any consistent recovery of data throughout the first part of the project was impeded by the grounding problem at the MARS node and only occasional ship operations over the site. The acoustically transmitted data records we were able to receive, each of 1–8 days' duration, show that the oceanographic sensors were powered hourly throughout the operational life of each BMFC and that they performed well (Fig. 4).

Both BMFCs took longer than initially expected to begin generating significant power to recharge the Li-ion batteries. The intermittent data collection leaves a range of time for this occurrence, between 22 and 84 days for BMFC 1 and 15–78 days for BMFC 2 (Fig. 5). This delay in the onset of significant power production can be attributed in large part to the increased chamber volume due to the compact clay deposit and the carbon-poor sediments at the field sites. The delay was in spite of the addition of gelatin blocks containing concentrated acetate to each chamber, which had been expected to help initiate the production of energy and to increase the overall output and duration of that energy production. In retrospect, this was not an ideal delivery method as the gelatin blocks had a tendency to break apart. Therefore, it is uncertain how much of the initial acetate/gelatin material arrived intact at the seafloor inside each anode chamber.

The osmopumps attached to each chamber collected and preserved small volume samples over a continuous

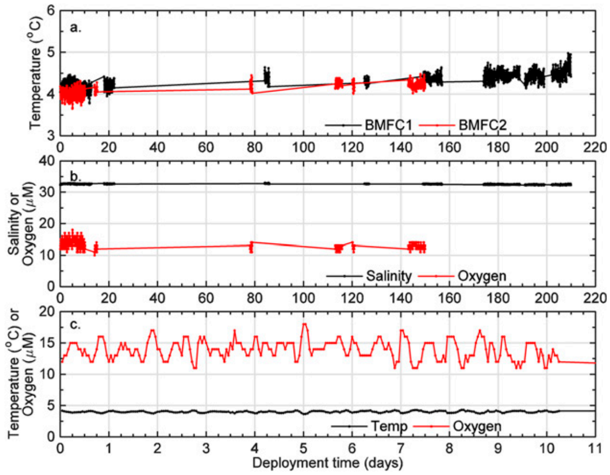

FIG. 4. Hourly oceanographic sensor readings of (a) temperature from BMFC 1 and BMFC 2, (b) salinity or oxygen concentration from BMFC 1 and BMFC 2, and (c) oxygen concentration and temperature from BMFC 2. These records reflect the data that were collected by acoustic transmission. The sensors were operational throughout the deployments.

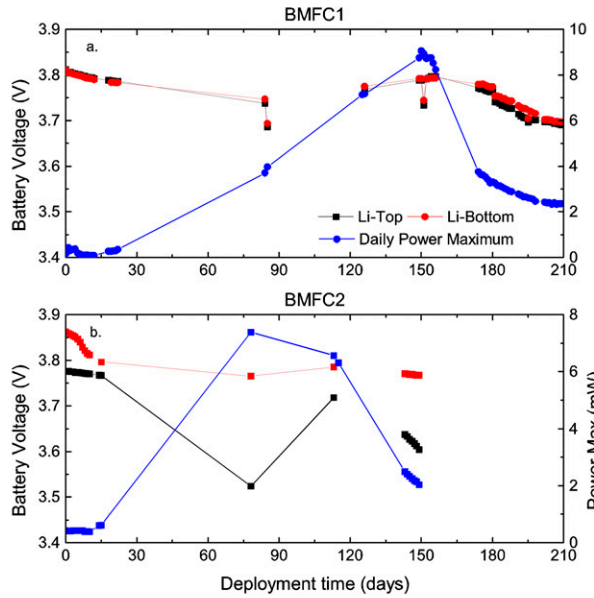

FIG. 5. Maximum power generation and voltages of the Li-ion battery stack for (a) BMFC 1 and (b) BMFC 2.

timeline throughout the entire deployment period. Half of these samples, amounting to collections approximately every 3–4 days, showed that in the anode chamber of BMFC 1, acetate concentrations were as high as 2 mM on day 6 and at or below 1 mM by day 18 (Fig. 6a). BMFC 2 had significantly more acetate within the chamber and for a longer period of time. Concentrations varied between 4 and 7 mM over the first 93 days before falling below 1 mM on day 107 for the remainder of the deployment.

The recovered records of energy generated from each BMFC are plotted in Fig. 7. BMFC 1 and 2 began producing modest amounts of energy 14 and 9 days after deployment, respectively. The net energy production of each fuel cell is represented by the total energy produced, less the energy required to operate the sensors, acoustic modem, PMP system, and its efficiency losses. The significant drops in net energy production on particular individual days are due to the energy-intensive acoustic communications that were undertaken on those same days. BMFC 1 generated a net surplus of energy on day 102 continuing until day 166 and remained operational for 210 days. BMFC 2 yielded a net surplus more than a month earlier on day 57 and was operational for 151 days. The shorter time required for BMFC 2 to begin producing surplus energy may have been partly due to the greater concentration of acetate within its anode chamber.

The shallow penetration depth of the anode chambers and the carbon-poor sediment likely contributed to a shorter-than-expected duration of BMFC operations as well as their slow start-up. Power production tapered off significantly by day 180 for BMFC 1 and day 156 for BMFC 2. Prior to these times, energy generation was sufficient to power not only the systems and oceanographic sensors, but also to restore the voltage of each of the stacked Li-ion batteries to a nearly fully charged state of 3.8 V—the notable exception being the Top cell in BMFC 2 (Fig. 5). A postrecovery analysis revealed that the Top Li-ion cell in BMFC 2 had unexpectedly failed, which on its own would have terminated the viability of this BMFC system. The PMP at this stage of development did not have any built-in redundancy, so the loss of one Li-ion cell was enough to cause the microcontroller to stop operating. The primary charge pump was directly controlled by the microcontroller. Therefore, even if the BMFC provided more energy, it was not harvested by the PMP. There were also periods of intense querying of both nodes owing to the problems associated with the modem attached to the MARS

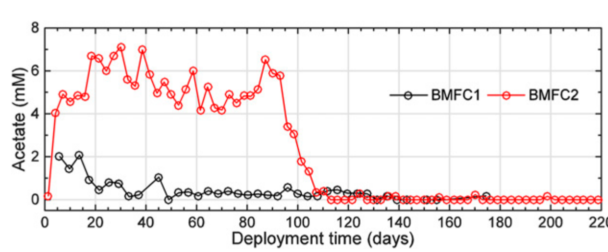

FIG. 6. Acetate concentrations (mM) in osmosampler coils from BMFC 1 and BMFC 2 during the deployment period.

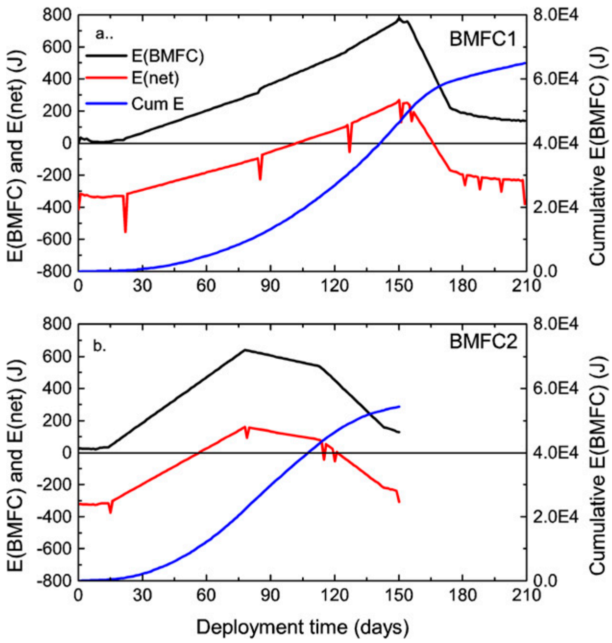

FIG. 7. Energy budgets for (a) BMFC 1 and (b) BMFC 2 showing total energy produced, both daily and cumulative, and net energy produced daily after accounting for the energy consumed by the PMP, modem, and sensor. Note that days with acoustic transmissions show dips in E(net).

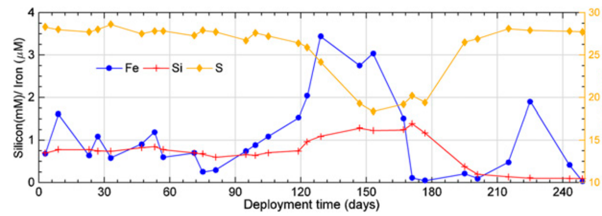

FIG. 8. ICP-AES chemical analysis of anode chamber fluid from BMFC 2 during the deployment period.

observatory. These queries may have contributed to the premature failure by unintentionally depleting stored energy reserves. The PMP did not have a fail-safe mechanism built in to automatically halt operations and go into a quiescent state until energy reserves were back above a specific level (although this fail-safe has since been added). Instead, if energy stores were entirely depleted, the system would have shut down and remained that way regardless of future energy production by the fuel cell.

d. *Chemical analysis and microbial community analysis*

The 300-m-long coil of tubing used to sample the internal fluid of the chambers combined with the sampling rate (1.4–2 days m^{-1}) yielded a chemical record throughout the duration of the deployment period. Half of these samples (representing every 3–4 days) were analyzed by ICP-AES. Analyses of the fluid in chamber 2 provide evidence that the chamber was sealed over the entire deployment and did not have any exchange of bottom water into the anode environment. Figure 8 shows the concentrations of total dissolved iron, sulfur, and silica over time within chamber 2. There are multiple instances where the concentration of sulfur (presumably as sulfate) decreases and the concentration of iron and silica increase during that same period. This was most pronounced between days 123 and 195. The increasing concentration of silica can most likely be attributed to an influx from benthic sources directly beneath the chamber. The changes in sulfur and iron concentrations were likely due to changes in speciation as both elements are reduced by biogeochemical processes in the enclosed chamber, on the anode surfaces, and in the underlying sediments. This could lead to elemental sulfur (S^0) deposits on the anode and various forms of iron [Fe(II) species], some of which are more soluble in seawater (Ryckelynck et al. 2005).

The ICP-AES data obtained from BMFC 1 displayed some similar trends but was deemed less reliable due to incomplete or discontinuous flushing of the sample coil. The problem was ascertained based on measured sodium concentrations as compared with those derived from salinity measurements in the same area. Sodium concentrations within the coil of BMFC 1 were diluted by 4%–15% compared to background seawater throughout the entire sampling period. Sodium concentrations within the coil of BMFC 2 were diluted by 0.3%–2.3%. Correction factors were applied to the chemical concentrations obtained by ICP-AES and to the acetate concentrations obtained by a separate assay to account for these effects.

Finally, bacterial community analyses of samples from the anode and underlying sediments of BMFC 2 at the order level reveal interesting trends (Fig. 9). These results confirm previous findings that showed a significant proportion of the sequences captured could be attributed to the phyla Bacteriodetes, Firmicutes, and Proteobacteria (Bond et al. 2002; Holmes et al. 2004; Nielsen et al. 2008; Reimers et al. 2007, 2013; White et al. 2009). Those three taxa represent 91% and 82% of the sequences found on the chamber 2 anode and sediment samples, respectively. The most striking of these results is the apparent enrichment of the Deltaproteobacteria Desulfobacterales going from 27% in the sediment to 59% on the anode. Desulfobacterales are strict anaerobes that obtain energy by reducing sulfate to sulfide, which may have played a role in the varying sulfur concentrations observed in the ICP-AES data. These results, along with visual evidence of much darker,

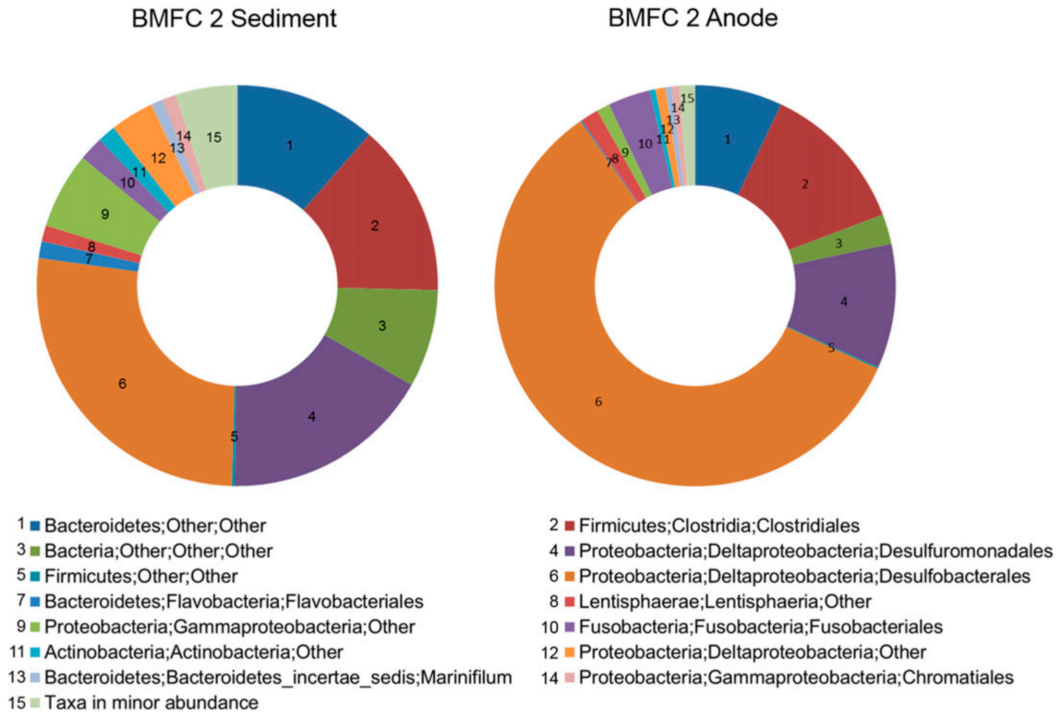

FIG. 9. Microbial community analysis of sediment and anode samples from BMFC 2 postrecovery.

nearly black, sediment inside both BMFCs upon being picked up by the ROV, imply that the redox conditions were still favorable for energy production after one year.

4. Discussion

While the total energy produced and the operational length of time were less than that achieved in other deployments of similar systems in nearshore tests, the maximum power generated (~9 mW) yields a power density of 35 mW m^{-2}, which is on the higher end of values reported in the literature for typical deployments (Bond et al. 2002; Gong et al. 2011; Nielsen et al. 2007; Reimers et al. 2001; Tender et al. 2002, 2008; Wotawa-Bergen et al. 2010). These results are highly encouraging given the general inhospitable nature of the deployment site in terms of low temperatures, low bottom water oxygen concentrations (affecting BMFC cathode reactions), low organic carbon content, and the physical makeup of the sediment. Furthermore, the duration of the functional life span of one of the fuel cell systems may have been shortened by a failing Li-ion cell linked to the PMP. Also, both systems, in an already low-energy potential environment, had abnormally high-energy burdens at times. There was a dramatic effect of acoustic communications on the net energy production as mentioned earlier and shown in Fig. 7. The communication difficulties led to a greater number of attempts at data retrieval in short windows of time, thereby depleting the available energy reserves of Li-ion batteries. It is possible that the PMP in each system was forced to shut down even though energy was still being harvested by the BMFCs. Upon recovery, observations of the sediment layer within each BMFC showed it to be a dark brown/black color, significantly darker than the surrounding sediment. This is likely due to iron sulfide mineral precipitation under anoxic conditions, indicating that the chamber maintained a reduced environment.

Both BMFCs were able to generate a surplus of power required by system components to perform scheduled tasks and remain functional. They were able to power environmental sensors and acoustic modems. Both systems also functioned autonomously and were able to both communicate and transfer data and information to either nearby ships on the surface (~0.9 km away) or directly to the MARS node (~0.5 km away). This dual functionality near the MARS observatory demonstrates the potential utility of these BMFC systems for network communications in deep-water settings. Individual units could be placed in remote locations with a variety of different sensors for regular relaying of environmental factors to a central gateway over the long term. Several systems could also be utilized together in an array to monitor larger areas, such as a regional oxygen minimum zone. In either situation, the gateway for communications and data retrieval could be via an observatory, mooring, autonomous underwater vehicle (AUV), or ship passing nearby. Modest improvements in efficiency, longevity, and reliability would also enable the potential use of BMFC systems as an inexpensive backup or alternative to solely battery-powered tsunami warning systems.

While the overall power production from each BMFC was modest relative to previous deployments, successful autonomous functionality and communications were important demonstrations. A key functional aspect of these units is to provide redundancy for power systems so as to not solely rely on batteries for energy demands. Simply increasing the size and/or number of batteries may not always be feasible for sensor systems. Larger batteries also carry a significantly greater risk of hazardous catastrophic failure, a noted significant concern of most government agencies, including the U.S. Office of Naval Research, which funded this work. Ideally, BMFCs allow small batteries to be selected such that their output can manage peak power demands for 2–3 days, while the BMFC provides sufficient energy to consistently recharge the batteries over the long term. Potential improvements that are likely to result in improved functionality described above include modifications to the PMP to improve efficiency and optimize data logging, and include a fail-safe mode to maintain operational viability in a low-energy state or unusually high-energy-demand situations. When future BMFC system demonstrations are planned, more attention will be given to predeployment site characterizations. Chambered BMFCs may also be preloaded with an internal layer of organic matter–enriched sediments instead of acetate to help prime the system and enable sustained maximum energy generation. The overall chamber design will also be improved to enable easier deployment and burial in a variety of sediment types.

Acknowledgments. We greatly thank Craig Dawe (MBARI technical support manager), Mike Burczynski, and D. J. Osborne (ROV *Ventana* pilots) for their valued input and efforts during deployment and recovery of the BMFCs on R/V *Point Lobos* and R/V *Rachel Carson*, and Stephanie Hillsgrove (Harvard University) for her efforts during recovery of the BMFCs. This work was funded by the Office of Naval Research under Grant N000140910199 to C. R.

REFERENCES

Altschul, S. F., W. Gish, W. Miller, E. W. Myers, and D. J. Lipman, 1990: Basic local alignment search tool. *J. Mol. Biol.*, **215**, 403–410, doi:10.1016/S0022-2836(05)80360-2.

Bond, D. R., and D. R. Lovley, 2003: Electricity production by *Geobacter sulfurreducens* attached to electrodes. *Appl. Environ. Microbiol.*, **69**, 1548–1555, doi:10.1128/AEM.69.3.1548-1555.2003.

——, D. E. Holmes, L. M. Tender, and D. R. Lovley, 2002: Electrode-reducing microorganisms that harvest energy from marine sediments. *Science*, **295**, 483–485, doi:10.1126/science.1066771.

Caporaso, J. G., and Coauthors, 2010: QIIME allows analysis of high-throughput community sequencing data. *Nat. Methods*, **7**, 335–336, doi:10.1038/nmeth.f.303.

Dewan, A., T. Ewing, M. E. Nielsen, C. E. Reimers, B. Chadwick, K. Richter, Z. Lewandowski, and H. Beyenal, 2010: Effect of location on the performance of benthic microbial fuel cells. *Proceedings of the Water Environment Federation: Biofilms 2010*, Vol. 2010, Water Environment Federation, Alexandria, VA, 48–51, doi:10.2175/193864710798208520.

Donovan, C., A. Dewan, D. Heo, and H. Beyenal, 2008: Batteryless, wireless sensor powered by a sediment microbial fuel cell. *Environ. Sci. Technol.*, **42**, 8591–8596, doi:10.1021/es801763g.

Girguis, P. R., and J. F. Holden, 2012: On the potential for bioenergy and biofuels from hydrothermal vent microbes. *Oceanography*, **25** (1), 213–217, doi:10.5670/oceanog.2012.20.

Gong, Y., S. E. Radachowsky, M. Wolf, M. E. Neilsen, P. R. Girguis, and C. E. Reimers, 2011: Benthic microbial fuel cell as direct power source for an acoustic modem and seawater oxygen/temperature sensor system. *Environ. Sci. Technol.*, **45**, 5047–5053, doi:10.1021/es104383q.

Hedges, J. I., and J. H. Stern, 1984: Carbon and nitrogen determinations of carbonate-containing solids. *Limnol. Oceanogr.*, **29**, 657–663, doi:10.4319/lo.1984.29.3.0657.

Holmes, D. E., D. R. Bond, R. A. O'Neil, C. E. Reimers, L. R. Tender, and D. R. Lovley, 2004: Microbial communities associated with electrodes harvesting electricity from a variety of aquatic sediments. *Microb. Ecol.*, **48**, 178–190, doi:10.1007/s00248-003-0004-4.

——, and Coauthors, 2006: Microarray and genetic analysis of electron transfer to elecrodes in *Geobacter sulfurreducens*. *Environ. Microbiol.*, **8**, 1805–1815, doi:10.1111/j.1462-2920.2006.01065.x.

Jannasch, H. W., C. G. Wheat, J. N. Plant, M. Kastner, and D. S. Stakes, 2004: Continuous chemical monitoring with osmotically pumped water samplers: OsmoSampler design and applications. *Limnol. Oceanogr. Methods*, **2**, 102–113, doi:10.4319/lom.2004.2.102.

Lovley, D. R., 2006: Bug juice: Harvesting electricity with microorganisms. *Nat. Rev. Microbiol.*, **4**, 497–508, doi:10.1038/nrmicro1442.

Nielsen, M. E., C. E. Reimers, and H. A. Stecher, 2007: Enhanced power from chambered benthic microbial fuel cells. *Environ. Sci. Technol.*, **41**, 7895–7900, doi:10.1021/es071740b.

——, ——, H. K. White, S. Sharma, and P. R. Girguis, 2008: Sustainable energy from deep ocean cold seeps. *Energy Environ. Sci.*, **1**, 584–593, doi:10.1039/b811899j.

Reguera, G., K. P. Nevin, J. S. Nicoll, S. F. Covalla, T. L. Woodard, and D. R. Lovley, 2006: Biofilm and nanowire production leads to increased current in *Geobacter sulfurreducens* fuel cells. *Appl. Environ. Microbiol.*, **72**, 7345–7348, doi:10.1128/AEM.01444-06.

Reimers, C. E., 2015: Applications of bioelectrochemical energy harvesting in the marine environment. *Biofilms in Bioelectrochemical Systems: From Laboratory Practice to Data Interpretation*, H. Beyenal and J. T. Babauta, Eds., Elsevier, 345–366, doi:10.1002/9781119097426.ch10.

——, L. M. Tender, S. Fertig, and W. Wang, 2001: Harvesting energy from the marine sediment-water interface. *Environ. Sci. Technol.*, **35**, 192–195, doi:10.1021/es001223s.

——, H. A. Stecher III, J. C. Westall, Y. Alleau, K. A. Howell, L. Soule, H. K. White, and P. R. Girguis, 2007: Substrate degradation kinetics, microbial diversity, and current efficiency of microbial fuel cells supplied with marine plankton. *Appl. Environ. Microbiol.*, **73**, 7029–7040, doi:10.1128/AEM.01209-07.

——, Y. Alleau, J. Bauer, J. Delaney, P. R. Girguis, P. S. Schrader, and H. A. Stecher, 2013: Redox effects on the microbial degradation of refractory organic matter in marine sediments. *Geochim. Cosmochim. Acta*, **121**, 582–598, doi:10.1016/j.gca.2013.08.004.

Ryckelynck, N., H. A. Stecher III, and C. E. Reimers, 2005: Understanding the anodic mechanism of a seafloor fuel cell: Interactions between geochemistry and microbial activity. *Biogeochemistry*, **76**, 113–139, doi:10.1007/s10533-005-2671-3.

Tender, L. M., and Coauthors, 2002: Harnessing microbially generated power on the seafloor. *Nat. Biotechnol.*, **20**, 821–825, doi:10.1038/nbt716.

——, and Coauthors, 2008: The first demonstration of a microbial fuel cell as a viable power supply: Powering a meteorological buoy. *J. Power Sources*, **179**, 571–575, doi:10.1016/j.jpowsour.2007.12.123.

Wang, Q., G. M. Garrity, J. M. Tiedje, and J. R. Cole, 2007: Naïve Bayesian classifier for rapid assignment of rRNA sequences into the new bacterial taxonomy. *Appl. Environ. Microbiol.*, **73**, 5261–5267, doi:10.1128/AEM.00062-07.

Wheat, C. G., H. W. Jannasch, A. T. Fisher, K. Becker, J. Sharkey, and S. Hulme, 2010: Subseafloor seawater-basalt-microbe reactions: Continuous sampling of borehole fluids in a ridge flank environment. *Geochem. Geophys. Geosyst.*, **11**, Q07011, doi:10.1029/2010GC003057.

White, H. K., C. E. Reimers, E. E. Cordes, G. F. Dilly, and P. R. Girguis, 2009: Quantitative population dynamics of microbial communities in plankton-fed microbial fuel cells. *ISME J.*, **3**, 635–646, doi:10.1038/ismej.2009.12.

Wotawa-Bergen, A. Q., D. B. Chadwick, K. E. Richter, L. M. Tender, C. E. Reimers, and Y. Gong, 2010: Operational testing of sediment microbial fuel cells in San Diego Bay. *Oceans 2010*, IEEE, 1–6, doi:10.1109/OCEANS.2010.5664612.